Supporting Information

A New Tunnel-Type V_4O_9 Cathode for High Power Density Aqueous Zinc Ion Batteries

*Qiaoran Wang, Tianjiang Sun, Shibing Zheng, Lin Li, Tao Ma, and Jing Liang**
E-mail: liangjing@nankai.edu.cn

Table of Contents

Fig. S1.........2

Fig. S2.........3

Fig. S3.........4

Fig. S4.........5

Fig. S5.........6

Fig. S6.........7

Fig. S7.........8

Fig. S8.........9

Fig. S9.........10

Fig. S10.........11

Fig. S11.........12

Fig. S12.........13

Fig. S13.........14

Fig. S14.........14

Fig S15.........15

Table S1.........15

Table S2.........16

Table S3.........16

Notes and references.........19

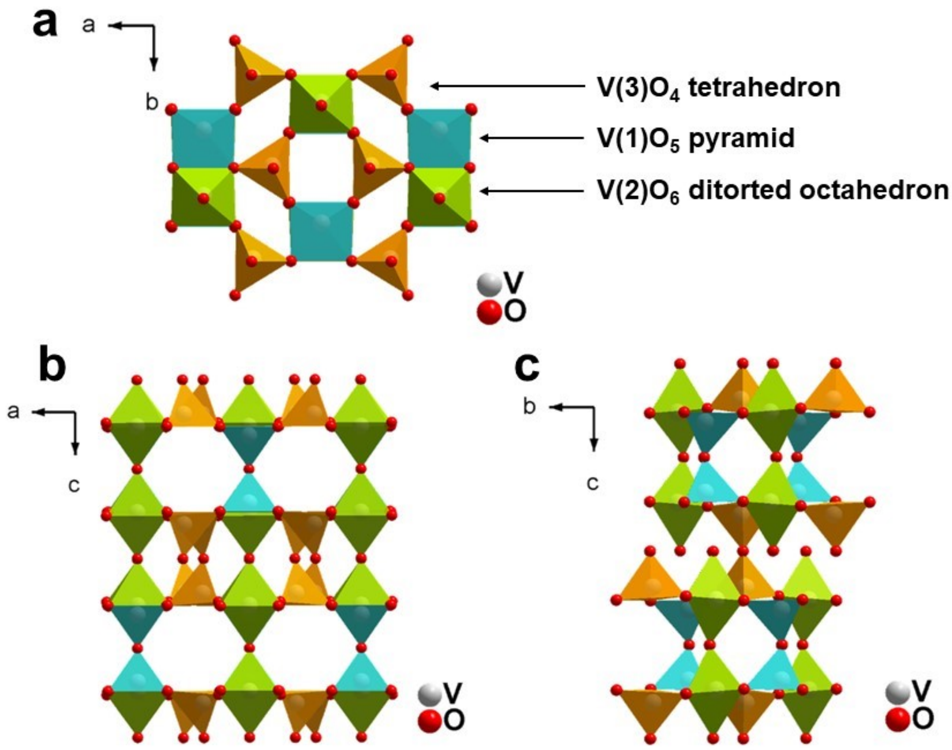

Fig. S1. Crystal structure along the (a) c-axis, (b) b-axis and (c) a-axis of the orthorhombic V_4O_9.

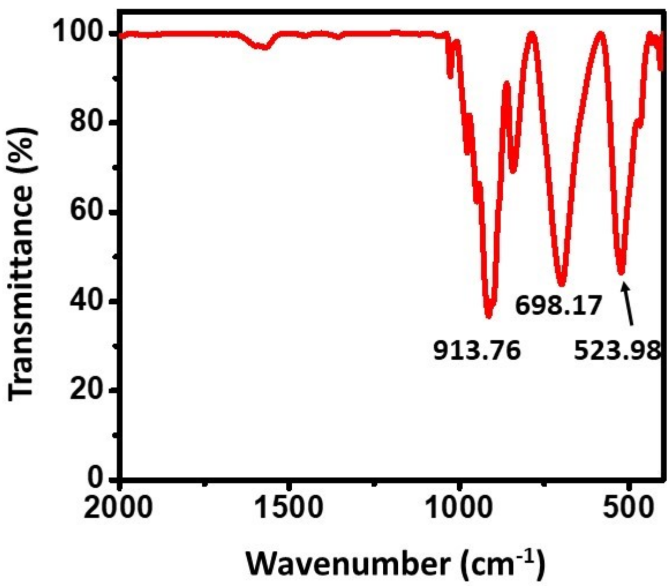

Fig. S2. FTIR spectrum of V_4O_9 at attenuated total reflection mode.

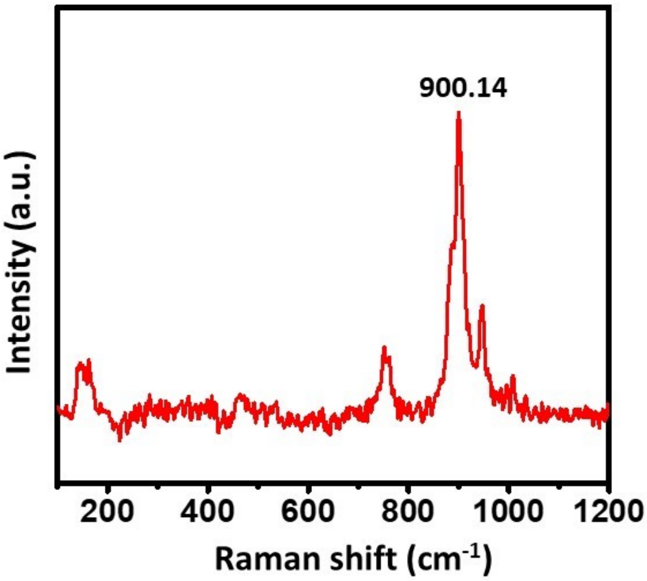

Fig. S3. Raman scattering of V_4O_9 powder.

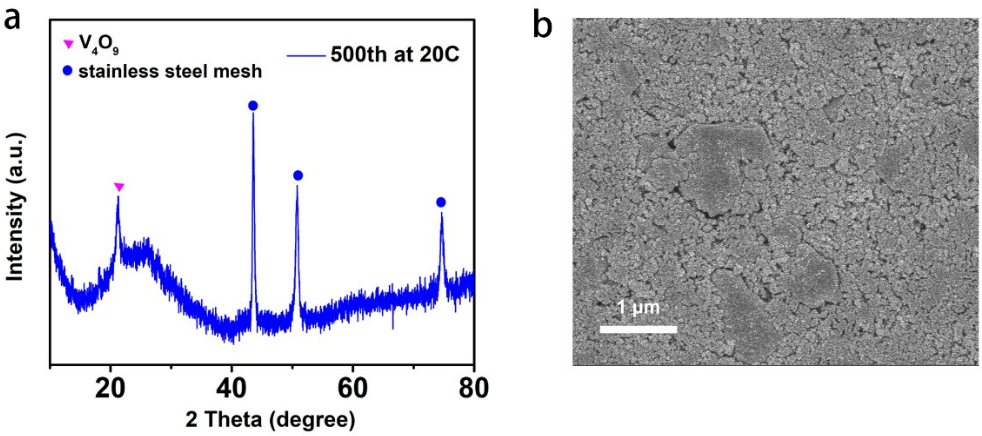

Fig. S4. (a) XRD and (b) SEM of V_4O_9 electrode after 500th at 20C

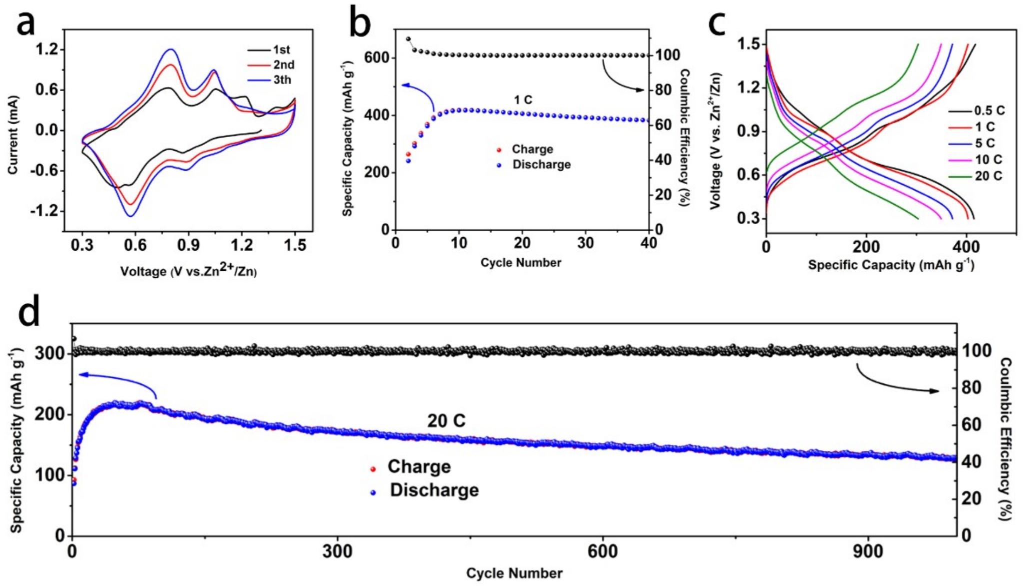

Fig. S5. Electrochemical performance of Zn/V_4O_9 with 3M ZnSO4 electrolyte. (a) The first three cyclic voltammetry (CV) profile of V_4O_9 at 0.5 mV s^{-1}. (b) Cycle performance at 1 C. (c) Charge/discharge profiles at 0.5 C, 1 C, 5 C, 10 C, 20 C. (d) Cycle performance at 20 C.

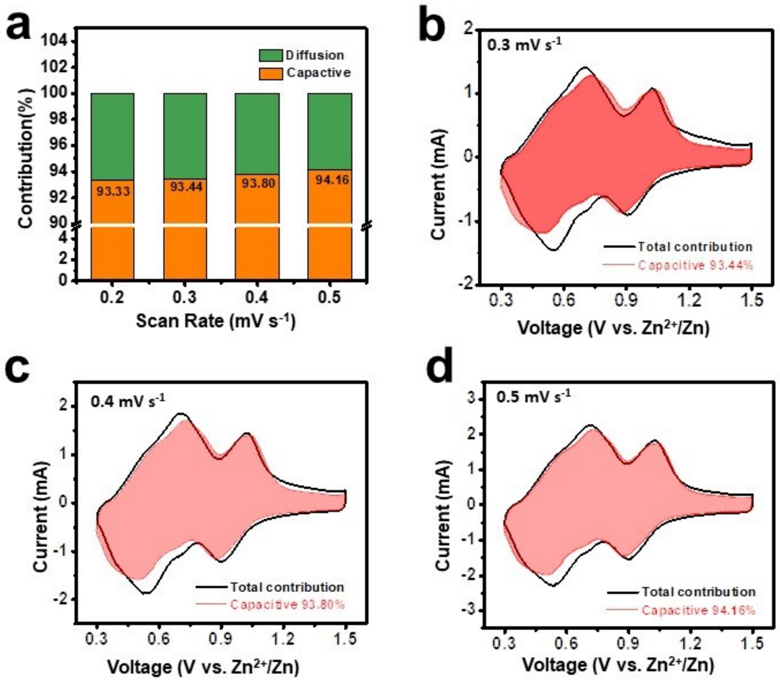

Fig. S6. (a) Percentages of capacitive and diffusion contributions at different scan rates. Contribution ratios of the capacitive capacities and diffusion-controlled capacities at (b) 0.3 mV s^{-1}, (c) 0.4 mV s^{-1} and (d) 0.5 mV s^{-1}.

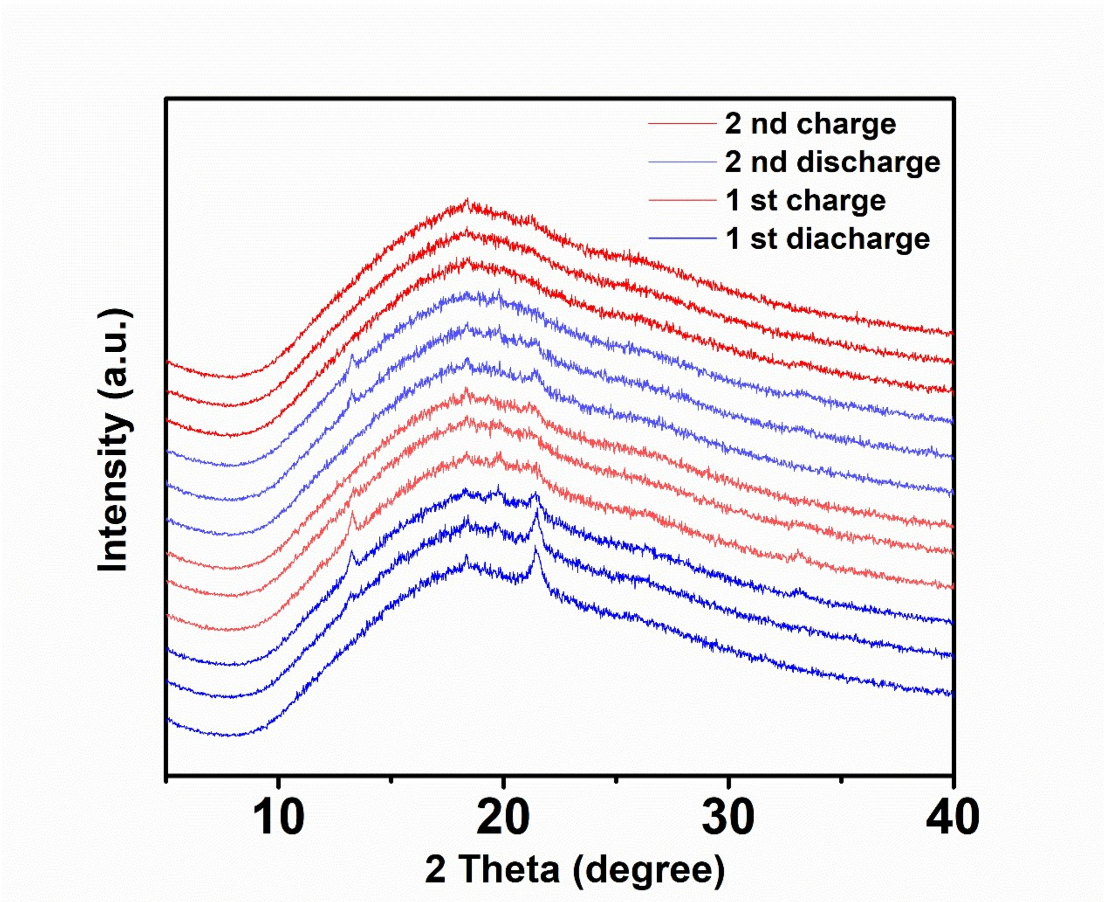

Fig. S7. In-situ XRD of V_4O_9 electrode at the first two cycles.

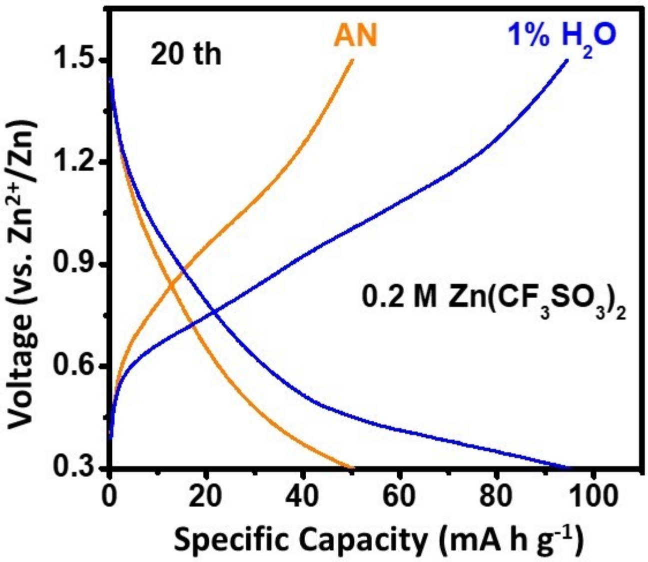

Fig. S8. Galvanostatic voltage–capacity profiles for V_4O_9 cycled in electrolytes without and with 1% content in 0.2 M $Zn(CF_3SO_3)_2$ acetonitrile (anhydrous). Each profile corresponds to the 20th cycle.

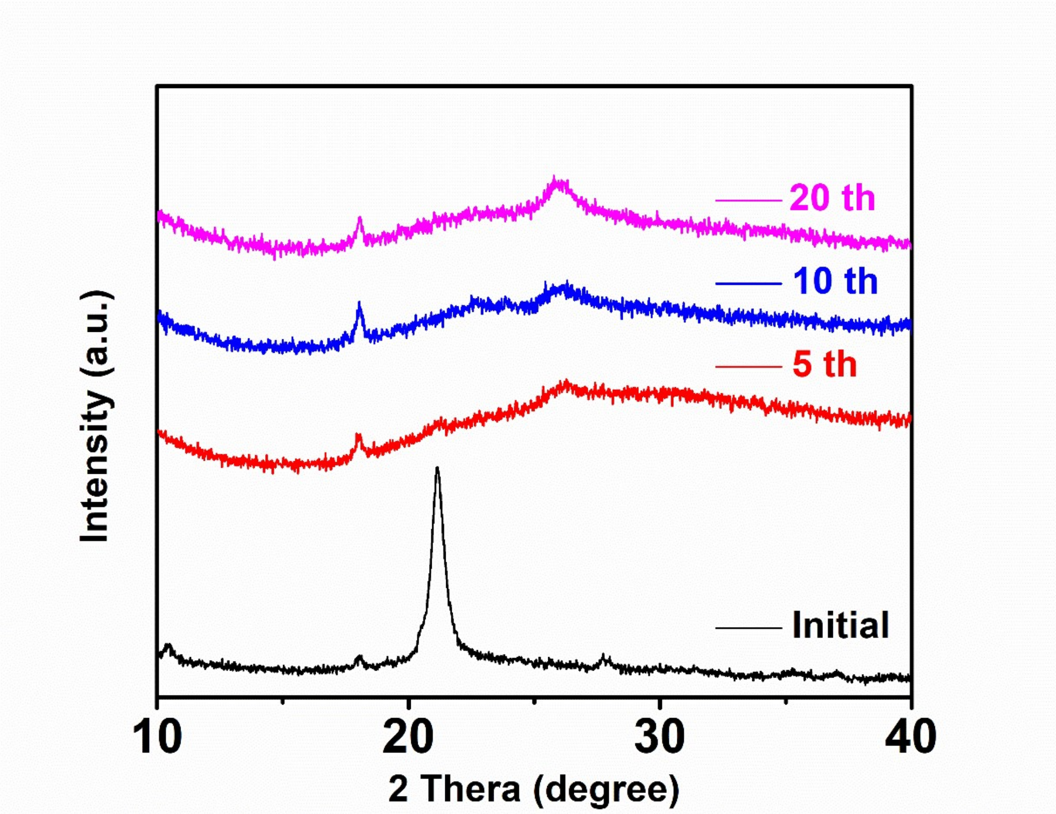

Fig. S9. XRD of V_4O_9 electrode at 5th, 10th, 20th at 1C.

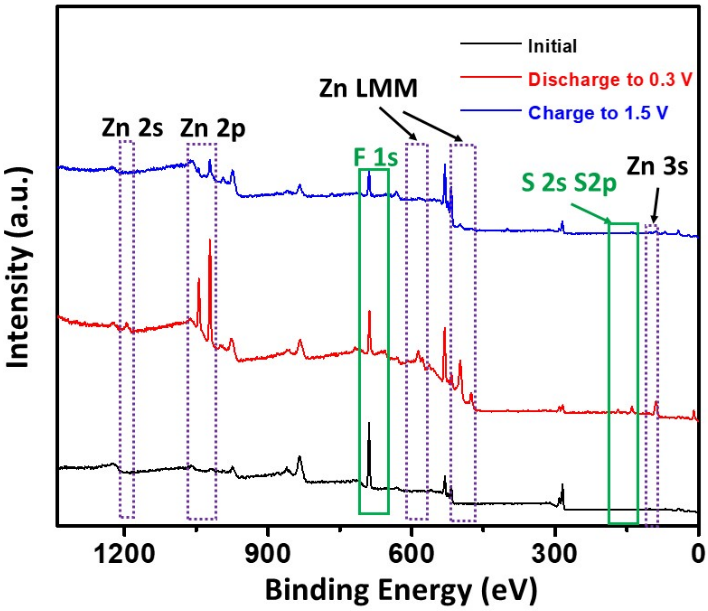

Fig. S10. XPS image of V_4O_9 electrodes at the initial, full discharging, and charging states.

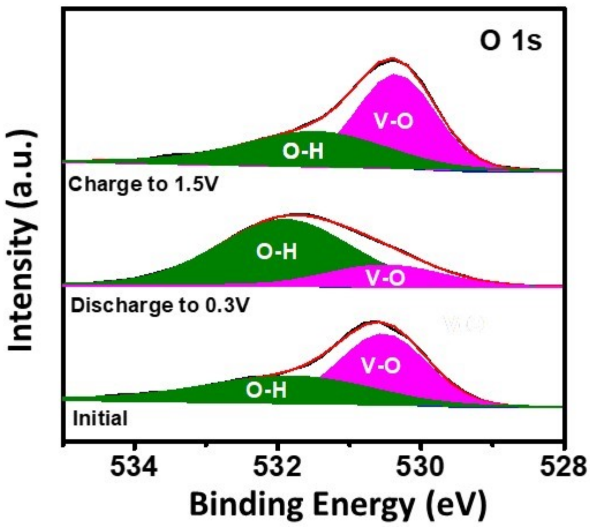

Fig. S11. Ex-situ XPS image of O 1s acquired from the pristine, full discharging, and charging V_4O_9 electrodes.

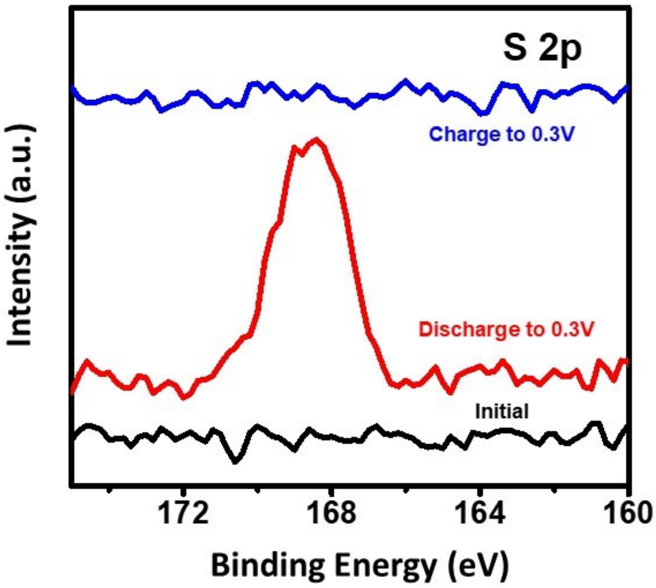

Fig. S12. Ex-situ XPS image of S 2p acquired from the pristine, full discharging and charging V_4O_9 electrodes.

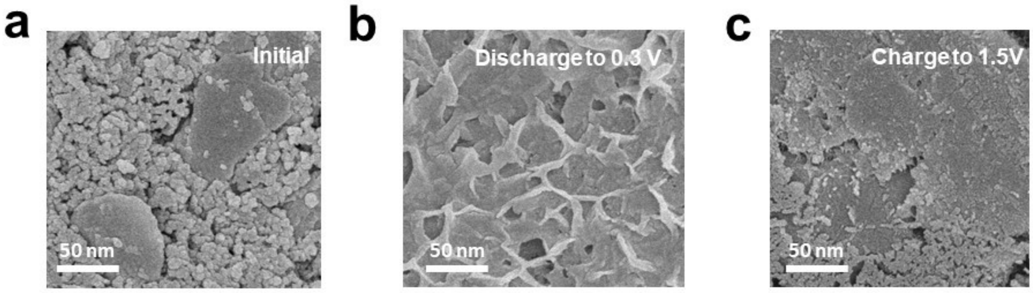

Fig. S13. SEM images of V_4O_9 electrodes at the (a) initial, (b) full discharging, and (c) charging states.

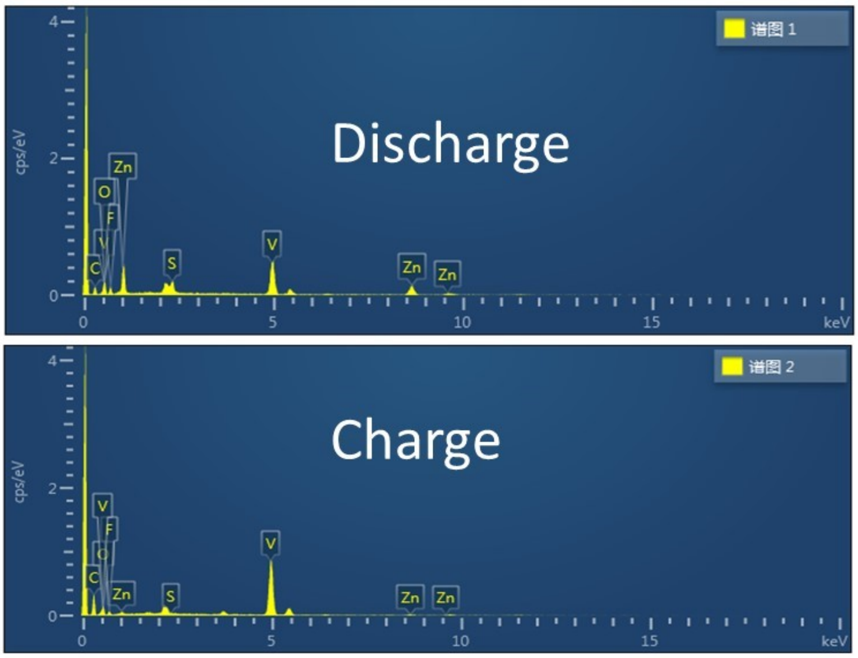

Fig. S14. EDX pattern of V_4O_9 electrode at the full discharging and charging states.

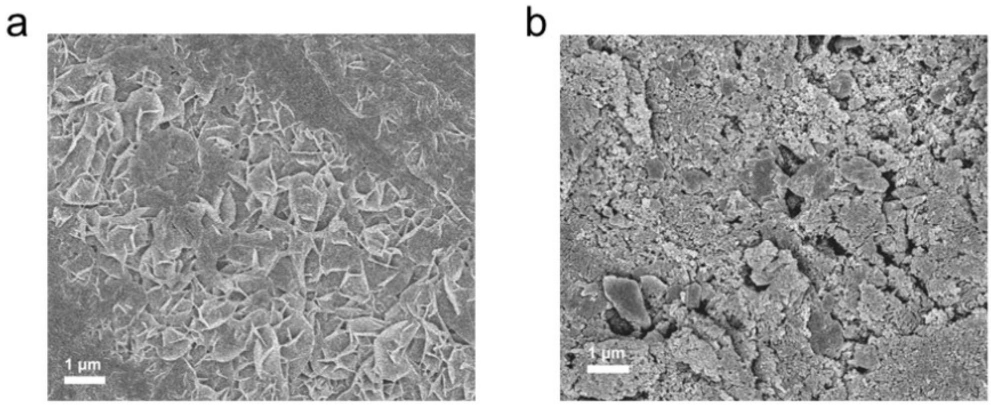

Fig S15. SEM of electrodes at the discharge state of 0.3 V without (a) and with (b) the treatment of dilute hydrochloric acid.

Table S1. Element distribution of V_4O_9 electrode at the full discharging and charging states.

	Discharge		**Charge**	
Element	**wt%**	**Atomic percentage**	**wt%**	**Atomic percentage**
C	18.00	34.89	29.50	50.29
O	20.31	29.55	17.78	22.75
F	11.73	14.37	8.82	9.50
S	2.73	1.98	0.00	0.00
V	23.76	10.86	41.89	16.83
Zn	23.46	8.35	2.01	0.63
Total:	100.00	100.00	100.00	100.00

Table S2 Element distribution of V_4O_9 at the discharge state of 0.3 V without and with the treatment of dilute hydrochloric acid.

	Without acid treatment		**With acid treatment**	
Element	**Apparent concentration**	**wt%**	**Apparent concentration**	**wt%**
C	1.90	15.32	6.64	30.63
O	4.15	17.73	1.72	11.58
F	4.39	10.06	4.46	14.25
S	0.66	1.25	0.00	0.00
V	15.83	28.07	23.03	42.95
Zn	14.87	27.57	0.30	0.60
Total:		100.00		100.00

Table S3. Electrochemical performance comparisons of V_4O_9 with other reported aqueous zinc ion batteries.

Cathode	**Electrolyte**	**Voltage window**	**Specific capacity/ Rate performance**	**Cycling performance**	**ref**
V_2O_5	3 M $Zn(CF_3SO_3)_2$	0.2-1.6 V	470 mA h g^{-1} at 0.2 A g^{-1} 396 mA h g^{-1} at 8.0 A g^{-1}	91.1% capacity retention over 4000 cycles at 5 A g^{-1}	1
V_2O_5/Graphene	3 M $ZnSO_4$	0.2-1.8 V	489 mA h g^{-1} at 0.1 A g^{-1} 123 mA h g^{-1} at 70 A g^{-1}	80% capacity retention after 3500 cycles at 30A g^{-1}	2
Porous V_2O_5	3 M $Zn(CF_3SO_3)_2$	0.5-1.5 V	226 mA h g^{-1} at 1 C 104 mA h g^{-1} at 10 C	81% capacity retention after 500 cycles at 2 C	3

V_2O_5 nanosheets	3 M $Zn(CF_3SO_3)_2$	0.3-1.6 V	452 mA h g^{-1} at 0.1 A g^{-1} 268 mA h g^{-1} at 30 A g^{-1}	92% capacity retention after 5000 cycles at 10A g^{-1}	4
PANI-intercalated V_2O_5	3 M $Zn(CF_3SO_3)_2$	0.2-1.6 V	375.2 mA h g^{-1} at 1 A g^{-1} 197.1 mA h g^{-1} at 20 A g^{-1}	97.6% capacity retention after 2000 cycles at 20A g^{-1}	5
VO_2(B)	3 M Zn $(CF_3SO_3)_2$	0.3-1.5 V	375 mA h g^{-1} at 0.25 C 171 mA h g^{-1} at 300 C	91.2% capacity retention after 300 cycles at 100 mA g^{-1}	6
VO_2(D)	3 M $ZnSO_4$	0.2-1.6 V	408 mA h g^{-1} at 0.1 A g^{-1} 200 mA h g^{-1} at 20 A g^{-1}	an attenuation rate of 0.0023% per cycle	7
VO_2(A)	3 M Zn $(CF_3SO_3)_2$	0.2-1.4 V	357 mA h g^{-1} at 0.1 A g^{-1} 165 mA h g^{-1} at 10 A g^{-1}	76% capacity retention over 500 cycles at 5 A g^{-1}.	8
$VO_2 \cdot 0.75H_2O$	3 M $ZnSO_4$	0.4-1.4 V	396 mA h g^{-1} at 0.05 A g^{-1} 88 mA h g^{-1} at 50 A g^{-1}	89% capacity retention over 1000 cycles at 10 A g^{-1}	9
VO_2(B)/RGO	3 M $Zn(CF_3SO_3)_2$	0.2–1.4 V.	456 mA h g^{-1} at 100 mA g^{-1} 292 mA h g^{-1} at 5 A g^{-1}	72% capacity retention over 1600 cycles at 5A g^{-1}	10
VO_2-PEDOT	3 M $Zn(CF_3SO_3)_2$	0.3-1.3V	448 mA h g^{-1} at 0.5 A g^{-1} 231 mA h g^{-1} at 10 A g^{-1}	84.5% capacity retention over 1000 cycles at 5 Ag^{-1},	11
$H_2V_3O_8$	3 M $Zn(CF_3SO_3)_2$	0.2-1.6 V	423.8 mA h g^{-1} at 0.1 A g^{-1} 113.9 mA h g^{-1} at 5.0 A g^{-1}	94.3% capacity retention after 1000 cycles at 5 A g^{-1}	12
$V_3O_7 \cdot H_2O$/rGO	1 M $ZnSO_4$	0.3-1.5 V	267 mA h g^{-1} under 1 C 85 mA h g^{-1} under 40 C	79% capacity retention over 1000 cycles at 5 C	13
V_6O_{13}	3 M $Zn(CF_3SO_3)_2$	0.2-1.5 V	360 mA h g^{-1} at 0.2 A g^{-1} 145 mA h g^{-1} at 24.0 A g^{-1}	92% capacity retention over 2000 cycles at 4 A g^{-1}	14

Od-V_6O_{13}	3 M $Zn(CF_3SO_3)_2$	0.2-1.5 V	401 mA h g^{-1} at 0.2 A g^{-1} 223 mA h g^{-1} at 5 A g^{-1}	86% capacity retention after 2000 cycles at 2 A g^{-1}	15
$V_6O_{13}\cdot nH_2O$	3 M $Zn(CF_3SO_3)_2$	0.2-1.4 V	395 mA h g^{-1} at 0.1 A g^{-1} 97 mA h g^{-1} at 20 A g^{-1}	87% capacity retention after 1000 cycles at 5A g^{-1}	16
CO_2 modified V_6O_{13}	3 M $Zn(CF_3SO_3)_2$	0.3-1.5 V	471 mA h g^{-1} at 0.1 A g^{-1} 175 mA h g^{-1} at 10 A g^{-1}	80% capacity retention after 4000 cycles at 2 A g^{-1}	17
$V_{10}O_{24}\cdot 12H_2O$	3M $Zn(CF_3SO_3)_2$	0.7-1.7 V	164.5 mA h g^{-1} at 0.2 A g^{-1} 80.0 mA h g^{-1} at 10 A g^{-1}	80.1% capacity retention after 3000 cycles at 10 A g^{-1},	18
V_2O_3@C	3 M $Zn(CF_3SO_3)_2$	0.3-1.5 V	350 mA h g^{-1} at 100 mA g^{-1} 250 mA h g^{-1} at 2 A g^{-1}	90% capacity retention over 4000 cycles at 5 A g^{-1}	19
V_4O_9	3 M $Zn(CF_3SO_3)_2$	0.3-1.5 V	420 mA h g^{-1} at 0.5 C 234.4 mA h g^{-1} at 50 C	78.8% capacity retention over 1000 cycles at 20 C	This work

Notes and references

1. N. Zhang, Y. Dong, M. Jia, X. Bian, Y. Wang, M. Qiu, J. Xu, Y. Liu, L. Jiao and F. Cheng, Rechargeable Aqueous Zn–V_2O_5 Battery with High Energy Density and Long Cycle Life, *ACS Energy Lett.*, 2018, **3**, 1366-1372.
2. X. Wang, Y. Li, S. Wang, F. Zhou, P. Das, C. Sun, S. Zheng and Z. S. Wu, 2D Amorphous V_2O_5/Graphene Heterostructures for High-Safety Aqueous Zn-Ion Batteries with Unprecedented Capacity and Ultrahigh Rate Capability, *Adv. Energy Mater.*, 2020, **10**, 2000081.
3. X. Chen, L. Wang, H. Li, F. Cheng and J. Chen, Porous V_2O_5 nanofibers as cathode materials for rechargeable aqueous zinc-ion batteries, *J. Energy Chem.*, 2019, **38**, 20-25.
4. X. Wang, L. Ma and J. Sun, Vanadium Pentoxide Nanosheets in-Situ Spaced with Acetylene Black as Cathodes for High-Performance Zinc-Ion Batteries, *ACS Appl. Mater. Interfaces*, 2019, **11**, 41297-41303.
5. S. Liu, H. Zhu, B. Zhang, G. Li, H. Zhu, Y. Ren, H. Geng, Y. Yang, Q. Liu and C. C. Li, Tuning the Kinetics of Zinc-Ion Insertion/Extraction in V_2O_5 by In Situ Polyaniline Intercalation Enables Improved Aqueous Zinc-Ion Storage Performance, *Adv. Mater.*, 2020, **32**, e2001113.
6. J. Ding, Z. Du, L. Gu, B. Li, L. Wang, S. Wang, Y. Gong and S. Yang, Ultrafast Zn^{2+} Intercalation and Deintercalation in Vanadium Dioxide, *Adv. Mater.*, 2018, **30**, 6.
7. L. Chen, Z. Yang and Y. Huang, Monoclinic VO_2(D) hollow nanospheres with super-long cycle life for aqueous zinc ion batteries, *Nanoscale*, 2019, **11**, 13032-13039.
8. R. Li, X. Yu, X. Bian and F. Hu, Preparation and electrochemical performance of VO_2(A) hollow spheres as a cathode for aqueous zinc ion batteries, *RSC Adv.*, 2019, **9**, 35117-35123.
9. N. Liu, X. Wu, L. Fan, S. Gong, Z. Guo, A. Chen, C. Zhao, Y. Mao, N. Zhang and K. Sun, Intercalation Pseudocapacitive Zn^{2+} Storage with Hydrated Vanadium Dioxide toward Ultrahigh Rate Performance, *Adv. Mater.*, 2020, **32**, e1908420.
10. F. Cui, J. Zhao, D. Zhang, Y. Fang, F. Hu and K. Zhu, VO_2(B) nanobelts and reduced graphene oxides composites as cathode materials for low-cost rechargeable aqueous zinc ion batteries, *Chem. Eng. J.*, 2020, **390**, 124118.
11. X. Liu, G. Xu, Q. Zhang, S. Huang, L. Li, X. Wei, J. Cao, L. Yang and P. K. Chu, Ultrathin hybrid nanobelts of single-crystalline VO_2 and Poly(3,4-ethylenedioxythiophene) as cathode materials for aqueous zinc ion batteries with large capacity and high-rate capability, *J. Power Sources*, 2020, **463**, 228223.
12. P. He, Y. Quan, X. Xu, M. Yan, W. Yang, Q. An, L. He and L. Mai, High-Performance Aqueous Zinc-Ion Battery Based on Layered $H_2V_3O_8$Nanowire Cathode, *Small*, 2017, **13**.
13. C. Shen, X. Li, N. Li, K. Xie, J. G. Wang, X. Liu and B. Wei, Graphene-Boosted, High-Performance Aqueous Zn-Ion Battery, *ACS Appl. Mater. Interfaces*, 2018, **10**, 25446-25453.
14. J. Shin, D. S. Choi, H. J. Lee, Y. Jung and J. W. Choi, Hydrated Intercalation for High-Performance Aqueous Zinc Ion Batteries, *Adv. Energy Mater.*, 2019, **9**, 1900083.
15. M. Liao, J. Wang, L. Ye, H. Sun, Y. Wen, C. Wang, X. Sun, B. Wang and H. Peng, A Deep-Cycle Aqueous Zinc-Ion Battery Containing an Oxygen-Deficient Vanadium Oxide Cathode, *Angew. Chem., Int. Ed.*, 2020, **59**, 2273-2278.
16. J. Lai, H. Zhu, X. Zhu, H. Koritala and Y. Wang, Interlayer-Expanded $V_6O_{13}\cdot nH_2O$ Architecture Constructed for an Advanced Rechargeable Aqueous Zinc-Ion Battery, *ACS Appl. Energy Mater.*, 2019, **2**, 1988-1996.

17. W. Shi, B. Yin, Y. Yang, M. B. Sullivan, J. Wang, Y. W. Zhang, Z. G. Yu, W. S. V. Lee and J. Xue, Unravelling V_6O_{13} Diffusion Pathways via CO_2 Modification for High-Performance Zinc Ion Battery Cathode, *ACS Nano*, 2021, **15**, 1273-1281.
18. T. Wei, Q. Li, G. Yang and C. Wang, High-rate and durable aqueous zinc ion battery using dendritic $V_{10}O_{24}\cdot 12H_2O$ cathode material with large interlamellar spacing, *Electrochim. Acta*, 2018, **287**, 60-67.
19. Y. Ding, Y. Peng, S. Chen, X. Zhang, Z. Li, L. Zhu, L. E. Mo and L. Hu, Hierarchical Porous Metallic V_2O_3@C for Advanced Aqueous Zinc-Ion Batteries, *ACS Appl. Mater. Interfaces*, 2019, **11**, 44109-44117.